J Nanopart Res (2013) 15:1428
DOI 10.1007/s11051-013-1428-5

RESEARCH PAPER

Fulvic acids concentration and pH influence on the stability of hematite nanoparticles in aquatic systems

Daniel Palomino · Serge Stoll

Received: 6 June 2012 / Accepted: 11 January 2013 / Published online: 20 January 2013

Abstract In aquatic systems, fulvic acids (FAs) are expected to play key roles on the stability and aggregation behavior of manufactured nanoparticles (NPs). The exact conditions under which aggregation or dispersion occurs will depend on the nanoparticle surface charge properties, FAs concentration as well as solution conditions, such as pH and ionic strength. The systematic calculation of stability (aggregation versus disaggregation) diagrams is therefore a key aspect in the prediction of the environmental fate and behavior of manufactured nanoparticles in aquatic systems. In this study, the responses to changes in pH and FAs concentrations on the resulting surface charge of purified iron oxide nanoparticles (53 nm nominal diameter) is investigated. By adjusting the pH, different nanoparticle surface charge electrostatic regions are found, corresponding to positively, neutral, and negatively charged nanoparticle solutions. For each situation, the adsorption of negatively charged FAs at variable concentrations is considered by analyzing surface charge modifications and calculating experimental kinetics aggregation rates. Results show that, under the conditions used, and range of FAs environmental relevant conditions, the nanoparticle aggregation process is promoted only when the nanoparticle positive surface charge (solution pH less than the charge neutralization point) is compensated by the adsorption of FAs. In all the other cases, FAs adsorption and increase of FAs concentration are expected to promote not only the NPs stabilization but also the disaggregation of NPs aggregates. In addition, our study suggest that very low concentrations of FAs >0.1 mg/l are sufficient to rapidly stabilize iron hydroxide NPs solutions at concentration <5 mg/l.

Keywords Iron oxide nanoparticles · Fulvic acids · Aggregation kinetics · Disaggregation · Nanoparticle stability

D. Palomino · S. Stoll (✉)
Group of Environmental Physical Chemistry,
F.-A. Forel Institute, University of Geneva, 10 route de Suisse, 1290 Versoix, Switzerland
e-mail: serge.stoll@unige.ch

Introduction

The understanding of the interaction processes between manufactured nanoparticles and aquatic compounds is essential to predict nanoparticle mobility, bioavailability and their physicochemical transformations in aquatic systems. Humic substances (HS) represent an active and important fraction of natural organic matter (NOM) in aquatic environments (Aiken 1985; Buffle et al. 1998) and play important roles in water quality for many pollutants such as trace metals, radionuclides, and organic compounds owing to their strong sorbent properties, small size, and high charge density (Averett 1995; Maurice and Namjesnik-Dejanovic 1999;

Murphy et al. 1990; Santschi 1984). HS are also expected to adsorb on mineral and colloid surfaces, including manufactured nanoparticles (NPs), and the resulting adsorption layers and surface modification to have a significant impact on their fate and circulation (Ju-Nam and Lead 2008; Tipping and Higgins 1982). Stabilized nanoparticles may be transported over long distances, whereas, unstable NPs may be trapped locally through aggregation and sedimentation processes. The exact composition of HS is still nowadays not clearly determined due to the high heterogeneity of the functional groups such as aromatic residues, aliphatic chains, carboxylic, phenolic, and alkoxy groups, however, HS can be categorized in three groups: fulvic acids (FAs) which are the major component and smallest structures of HS and soluble at any pH, humic acids (HA) which represent bigger structures that are insoluble at $pH < 2$ and finally Humin which is insoluble at any pH (Jones and Bryan 1998; Piccolo 2001). Iron oxides are found naturally in the environment and play important roles on many biological processes (Stemmler and Berthelin 2003). More particularly, in fresh water systems, Hematite is found as one of the most abundant iron sources (Buffle et al. 1988; Stumm and Morgan 1996). Iron oxides nanoparticles are also willing to be used in many applications such as nanomedicine and imaging (Gupta and Gupta 2005), food industry (Fidler et al. 2004), waste water treatment (Cross et al. 2009; Perez 2007), and in soil remediation processes (Watts et al. 1997; Zhang 2003; Waychunas et al. 2005; Shipley et al. 2010) to remove chlorinated organic compound, and highly toxic heavy metals such as lead, cadmium, arsenic, etc. Owing to the multitude of potential environmental nanoparticle applications, manufactured nanoparticle quantities which can enter directly the environment are thus important. The extent to which manufactured NPs agglomerate will depend, besides the processing conditions, on the balance between the attractive and repulsive forces among the nanoparticles as well as between them and the environmental matrix mobilizing agents. The exact impact of such nanoparticles in environmental systems could also be difficult to estimate in particular in the case of soil remediation applications where the transport and fate of the injected nanoparticles are difficult to monitor (Kadar et al. 2010).

The stability and transformation of released NPs with regards to aggregate formation or propensity to form complexes (Carnal and Stoll 2011; Ferretti et al. 2003; Liang and Morgan 1990; Tipping and Higgins 1982) with water components is then a key aspect in investigating the fate of these materials. Several studies have shown that dissolved organic matter, ionic strength, pH, solution properties have important impacts on the stability of nanoparticles in aquatic systems. In particular, (Baalousha 2009) investigated the influence of pH and standard Suwannee river humic acids (SRHA) on the aggregation and surface properties of unpurified iron oxide manufactured nanoparticles. Iron oxide NPs were shown to form increasingly large aggregates with the increase in both pH (from 2 to 6) and SRHA concentration (from 0 to 25 mg/l) with the formation of open, porous aggregates in the absence of SRHA and compact aggregates in the presence of SRHA. The aggregation behavior of iron oxide NPs at variable concentrations of NPs and SRHA, and the disaggregation behavior of iron oxide aggregates in the absence and presence of SHRA were also investigated (Baalousha et al. 2008). The effect of FAs adsorption on the aggregation kinetics and fractal dimension of hematite particle aggregates was investigated in (Amal et al. 1992) at constant pH (pH 3). It was shown that the fractal dimensions of hematite aggregates partially coated with FAs were higher than those obtained with no adsorbed FAs. Computer simulations were also used (Seijo et al. 2009) to study the interactions of FAs with hematite particles to get an insight into the global effect of the electrostatic repulsive and attractive interactions, at pH 8, on the amount of adsorbed FAs and resulting structure of the adsorbed layer. Results demonstrated that the amount of adsorbed FAs was largely controlled by the solution ionic strength, FAs coagulation in solution may strongly compete with FAs adsorption at the hematite surface, and that the adsorption of large quantities of FAs at the NPs surface was not necessary leading to the formation of a homogeneous compact adsorbed layer.

Despite the importance of pH in controlling the NPs surface charge density as well as NPs surface charge (positive, neutral or negative) modification, surface transformation (and thus chemical reactivity) due to the presence of NOM, few studies have been performed to determine the stability diagram of iron oxide NPs (Amal et al. 1992; Baalousha 2009;

Baalousha et al. 2008; Seijo et al. 2009). In this paper, the stability diagram of purified hematite nanoparticles is determined as a function of two variable parameters, the pH and FAs concentration. Focus is made on the importance of the electrostatic interactions, surface charge compensation, and charge inversion effects. Three electrostatic "regimes" are investigated; (i) positively charged hematite particles interacting with negatively charged FAs, (ii) uncharged hematite particles interacting with negatively charged FAs and (iii) negatively charged hematite particles interacting with negatively charged FAs. The FAs concentration is adjusted (by adding successive amounts of FAs to the solutions) for each regime to study surface charge variations and effects on the NPs stability via the calculation of kinetics aggregation rates.

Materials and methods

Hematite synthesis

Two litres of HCl 2×10^{-3} M solution prepared with MilliQ water with a maximum resistivity of 18 MΩ·cm^{-1} and analytical grade HCl 35 % from Sigma–Aldrich has been heated to 98 °C in a SHOTT 2 l flask. After temperature stabilization, 5.408 g of $FeCl_3 \cdot 6H_2O$ were added into the solution. The mixture was then maintained at 98 °C in the closed flask during 10 days (He et al. 2007; Schwertmann and Cornell 1991). The solution was then cooled at room temperature and the mixture dialyzed with SpectrumLabs SpectraPor 12–14 kDa dialysis membranes rolls to remove all the ionic dissolved substances (especially iron chloride) remaining in the solution after the synthesis. Several dialyses were necessary to reach similar low conductivity as MilliQ water. The synthesized hematite (α-Fe_2O_3) NPs were stored in a cool and dark place. The nanoparticle concentration was then calculated by determining the molar extinction coefficient (4.06×10^3) according to (Schwertmann and Cornell 1991) based on the absorbance at 385 nm of different concentration suspensions using a HACH Lange DR-3800 spectrophotometer. The concentration was found equal to 1.64 ± 0.04 g/l in agreement with the concentration given in (He et al. 2007).

The synthesized nanoparticles (pH = 3) were placed on an aluminum stub covered with a 5 × 5 cm silica wafer from Agar Scientific (G3390). 2–3 nm gold coating was used to have the best contrast on a JEOL JSM-7001FA scanning electron microscope (SEM). Hematite nanoparticle images (Fig. 1a) and size measurements were conducted under high vacuum. After image analysis of more than 50 SEM pictures, the mean SEM diameter of the individual nanoparticles was found equal to 53 ± 5 nm confirming that the nanoparticle sizes were reasonably monodisperse. Zeta potential and sizes were also measured using a Malvern ZetaSizer Nano ZS. The Z-average hydrodynamic diameter was found equal to 94 ± 3 nm at pH = 3, indicating the presence of dimmers and trimers in solution, and the zeta-potential value was found equal to +45 ± 4 mV. The NP solutions were found stable for pH values less than 6.

Suwannee river fulvic acids preparation

Fulvic Acids were provided as a dehydrated powder by the International Humic Substances Society (Suwannee River Fulvic Acid Standard, II, 2S101F). 100 mg/l stock solution of FAs was prepared, and then pH adjusted to 10 and stirred over 24 h at 600 rpm to improve the solution stability. The solution was then protected from light and maintained between 0 and 5 °C.

Preparation of the hematite-FAs mixtures

Experiments were performed in a 150 ml polyethylene beaker. 200 µl of the Hematite NPs stock solution were added to milliQ water and pH adjusted. Then, the FAs volume was adjusted to obtain the desired concentration, and pH, using a 100 mg/l stock solution stirred 30 min at 800 rpm before use. The total volume was equal to 100 ml with a NPs nominal concentration equal to 3.28 mg/l and the solution was stirred at 200 rpm. The aggregation kinetics rates were calculated by measuring the aggregate size evolution as a function of time (0, 10, 20, 30, 40, 60, and 90 min). For that purpose, DLS measurements were performed with a Malvern Nano ZS equipped with a 633 nm He–Ne laser and operating at an angle of 173°. Then a linear regression analysis on all the data over 90 min was performed to obtain the mean size variation with time. The zeta potential was also measured on the

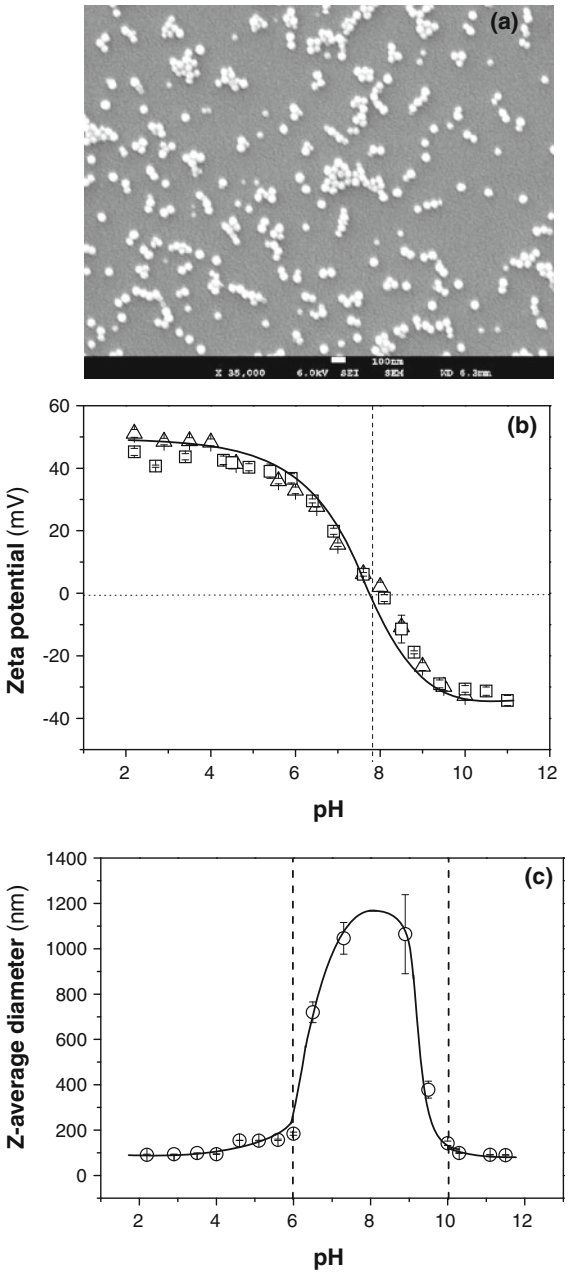

Fig. 1 **a** SEM image showing the monodispersity of our synthesized hematite NPs. **b** Zeta-potential evolution as a function of pH indicating that the NPs PZC (charge neutralization point) is equal to pH 8.0. *Triangle* represents the zeta-potential values obtained by a pH titration process from 2 to 10, and *square* for a titration process from 10 to 2. **c** Size evolution as a function of pH indicating that the aggregation region is comprised between pH 6 and 10

same apparatus using a combination of laser Doppler velocimetry and phase analysis light scattering at the same time intervals to correlate the surface charge variation with the aggregation kinetics. Each sample was analyzed three times.

Results and discussions

Hematite characterization as a function of pH

To get an insight on the surface charge pH dependence and resulting stability of the NPs in solution, pH titration curves were first determined. As shown in Fig. 1b, the NPs exhibit a stable and positive charge from pH 2 to 4 (+48 mV). Then the charge decreases to pass the point of zero charge (PZC) at pH 8.0 in good agreement with the values reported in the literature (Chen et al. 2006; Kosmulski 2002; Zhang and Buffle 1995). By increasing further the pH, the surface charge becomes negative. The negative charge is found to stabilize at -30 mV at pH 10. In parallel, the Z-average diameter evolution with pH was determined (Fig. 1c) and the size was found stable from pH 2 to 4 with an average diameter equal to 95 ± 3 nm. Then the size was found to increase to reach a maximum around the PZC with values greater than 1,000 nm indicating strong aggregation. At high pH values (pH > 10), the average diameter was found to reach a stable value equal to 93 ± 5 nm. It is important to note here that the Z-average diameter variations are the result of 2 titration curves: the first one from pH 2 to 8 and the second one from 11 to 8. Indeed, when passing the PZC, aggregates which are formed in the PZC region do not disaggregate by further increasing the pH. Once formed, the surface charging process and charge inversion of the NPs is not strong enough from an electrostatic point of view to re-disperse again the NPs.

Fulvic acids characterization as a function of pH

FAs zeta-potential variations as a function of pH are shown in Fig. 2. No PZC is observable for these compounds; they remain negatively charged even at low pH values. By increasing the pH, the zeta-potential value decreases from −35 mV down to −60 mV with a zeta potential equal to −58 mV at the corresponding hematite nanoparticles PZC. It should be noted at this point that, according to the calculated zeta-potential values for both the hematite NPs and FAs, different "electrostatic" regimes of possible interaction processes can be defined. The first

one is considering the most favorable scenario; positively charged NPs in the presence of negatively charged FAs which are expected to result in fast FAs adsorption at the NPs surface. The second one is considering the interaction of negatively charged FAs with uncharged hematite NPs, whereas the last one considers interactions between negatively charged species, hence corresponding to the most unfavorable case for FAs adsorption at the NPs surfaces. The different regimes are investigated below with variable FAs concentrations.

NPs stability as a function of FAs concentration: pH < PZC (pH 8)

To determine the aggregation kinetics rates for each FAs concentration, the NPs size evolution with time is measured and the variation of the Z-average (δRh) with time (δt) is calculated at pH = 4. If the solution is stable with time, δRh will be zero and if the solution is not stable the slope δRh/δt will be positive and proportional to the aggregation kinetics rate. In Fig. 3, the corresponding slope values are reported as a function of the FAs final concentrations. The solution is found monodisperse and stable in the absence of FAs, then in presence of FAs, three distinct behaviors are obtained: (a) from 0 to 0.03 mg/l, the NPs solution remains stable, (b) from 0.04 mg/l of FAs there is a rapid increase in the aggregation rate to reach a maximum value at 0.06 mg/l, (c) then by increasing further the FAs concentration a rapid decrease is observed and the NPs solution is found stable again between 0.1 and 0.5 mg/l. In the inset of Fig. 3, the corresponding zeta-potential values are also reported. Three distinct behaviors are also visible: (a) at low FAs concentration NPs remain positively charged with zeta-potential values greater than +10 mV, (b) by increasing the FAs concentration, the surface charge reaches a region in which the zeta potential is comprised between +10 and −10 mV and such a decrease of the NPs surface charge results in fast aggregation rates, (c) by increasing further the FAs concentration, charge inversion after reaching an equilibrium value is obtained thus preventing aggregation. It is important to note here that in comparison to the NPs charge inversion obtained by the successive increasing of the pH value above the PZC value for which only partial aggregate disaggregation is observed, the NPs charge inversion induced by the successive addition of FAs and adsorption was found very efficient to promote the dispersion of individual NPs and aggregate disaggregation.

NPs stability as a function of FAs concentration; pH = PZC

In this situation, the NPs surface charge is close to zero and thus the successive addition and adsorption of FAs at the NPs surface is normally expected to lead to the

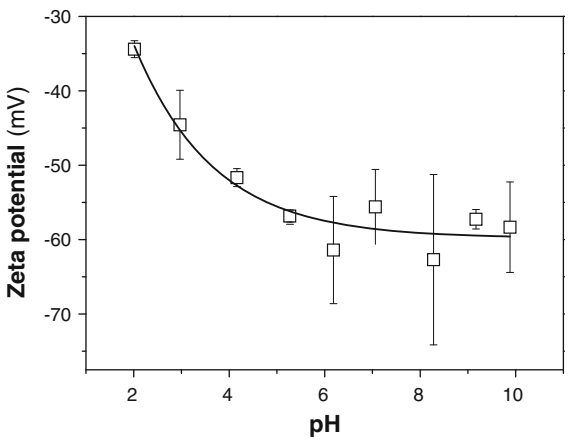

Fig. 2 FAs (50 mg/l) zeta-potential variation as a function of pH. FAs are found negatively charged for pH values ranging from 2 to 10

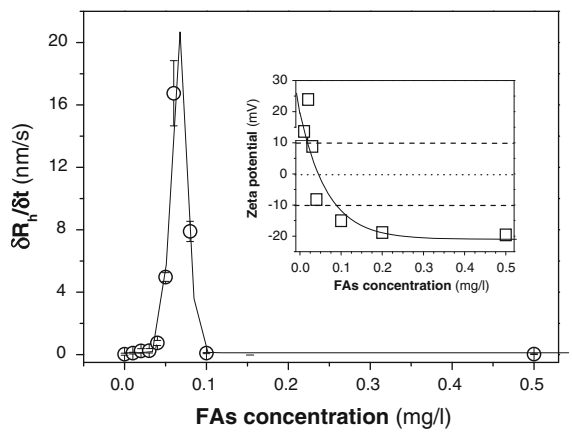

Fig. 3 Kinetics aggregation rates variation as a function of the FAs concentrations (0.01, 0.02, 0.03, 0.04, 0.05, 0.06, 0.08, 0.1, 0.5 mg/l) when pH < PZC (i.e., in the presence of negatively charged FAs and positively charged NPs). The curve was fitted with a Gaussian function with a maximum value found at 0.06 mg/l, corresponding to the FAs concentration required for the surface charge neutralization of the NPs as shown in the *inset*

formation of negatively charged complexes. This is clearly demonstrated in the inset of Fig. 4 by considering the zeta-potential variation as a function of FAs concentration. The NPs surface charge is found to rapidly decrease and stabilize to −40 mV. On the other hand, the δRh/δt variation indicates rapid stabilization of the NPs solution even at the lowest FAs concentration. It should be noted here that the FAs adsorption induces a strong variation of the NPs zeta-potential down to −45 mV, hence denoting strong interactions between NPs and FAs. It should be noted here that such a value is significantly more negative than the NPs zeta-potential values obtained in the absence of FAs and when pH was greater than the PZC value (see Fig. 1b).

NPs stability as a function of FAs concentration: pH > PZC

In the absence of FAs, at pH = 10, the NPs exhibit a negative value and the aggregation rate constant is zero. According to Fig. 5, adding FAs does not promote NPs aggregation, as expected. However, it is important to note here, as shown in the inset of Fig. 5, that the zeta-potential value obtained for the highest FAs concentration is more negative (−46 mV) than the one obtain at the same pH with NPs only (−35 mV). This indicates clearly that despite the fact that both NPs and FAs are negatively charged, FAs adsorption is still achieved, as observed in (Amal et al. 1992) and promotes an overcharging process at the NPs surface. It should be noted that the final zeta-potential value is comparable to the maximum zeta-potential value obtained at the PZC in the presence of FAs.

The determination of predictive diagrams is an important tool for the analysis of the surface charge transformation, stability and aggregation behavior of NPs in various environments in responses to changes in pH and FAs concentrations. As shown in the schematic stability diagram in Fig. 6, there is a complex and nonlinear interplay between the pH and the FAs concentration. Dashed areas representing the pH versus FAs concentration regions in which aggregation is observed clearly indicate that only two aggregation regions are possible; (i) at the NPs pH point of charge neutralization in the absence of FAs, and (ii) when NPs charge neutralization is achieved by FAs adsorption in the pH domain where the NPs are positively charged. In all the other cases FAs adsorption and further increases of FAs concentration are expected to promote the hematite NPs stabilization and NPs aggregate disaggregation.

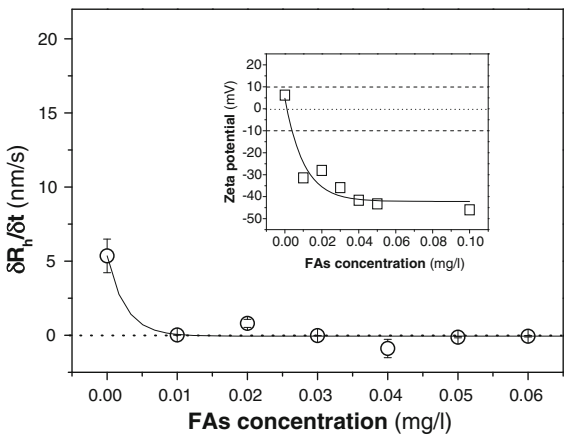

Fig. 4 Kinetics aggregation rates variation as a function of the FAs concentration when pH = PZC. The aggregation rate constant is rapidly going to zero at low FAs concentration. In the absence of FAs, NPs aggregation is observed (at the PZC). This rate is much lower than the one obtained at pH 4 with 0.06 mg/l of FAs corresponding to charge neutralization. The corresponding zeta-potential values given in the *inset* indicate that the NPs become rapidly negatively charged even in the presence of low FAs concentrations

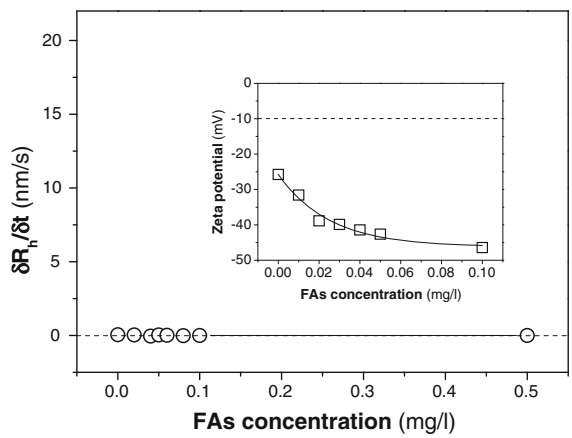

Fig. 5 Kinetics aggregation rates variation as a function of FAs concentration when pH > PZC. The aggregation rate constant is zero in the presence or absence of FAs. The zeta-potential values are decreasing from −25 mV to a maximum value of −45 mV indicating that a given amount of negatively charged FAs are adsorbed at the surface of the NPs

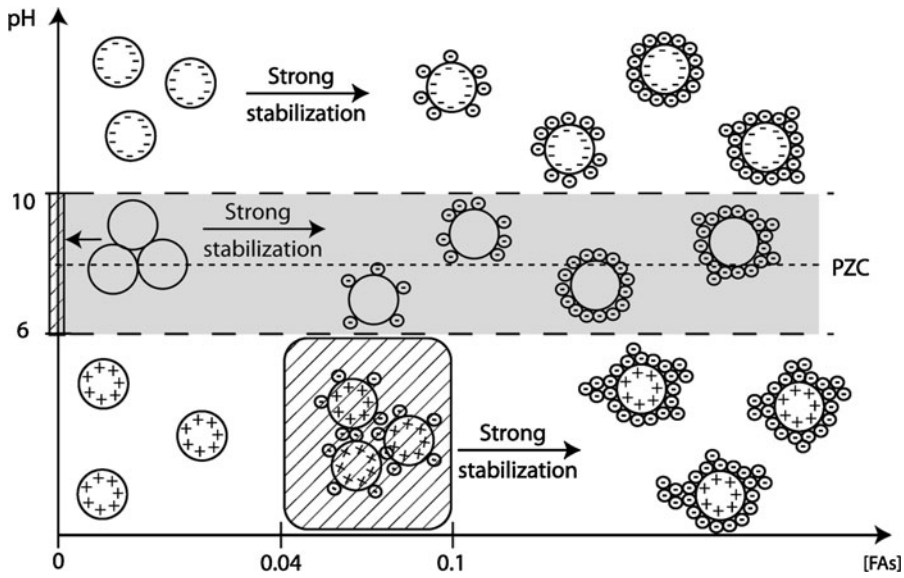

Fig. 6 Schematic stability diagram of Hematite NPs (3.28 mg/l) as a function of pH and FAs concentrations. Only two NPs aggregation domains can be defined here; (i) in the absence of FAs at the NPs point of zero charge, (ii) below the NPs point of zero charge and in a region where the positive NPs surface charge are compensated by the negatively charged FAs adsorption. In the other cases, the presence of FAs is found to stabilize and/or disaggregate the NPs

Conclusions

Our results clearly indicate that the aggregation of hematite nanoparticles is promoted by the adsorption of FAs only when the nanoparticle surface are positively charged, while in other cases, increasing adsorption of FAs results in the stabilization of hematite nanoparticles and disaggregation of hematite nanoparticle aggregates. Our study hence suggest that very low concentrations of FAs (>0.05 mg/l) are sufficient to rapidly stabilize iron hydroxide nanoparticles at concentration less than 5 mg/l, independent of the pH of the solution, and that FAs play important roles in the dispersion of already formed NPs aggregates. In all cases the negatively charged FAs adsorb on positive, neutral, and negative charged NPs, respectively. This indicates that the driving force for FAs adsorption is a combination of electrostatic attractive interactions between the FAs and the NPs, electrostatic repulsive interactions between the FAs at the NPs surfaces, specific chemical interactions, van der Waals, and hydrophobic interactions. Steric effects at the NPs surface are also playing key roles in the NPs stability. The results show that the times required to reach saturation of hematite NPs surface are short, much shorter that those typically expected and encountered in coagulation of inorganic colloids and when using linear polyelectrolyte chains in the stabilization and destabilization of colloidal suspensions (Ouali and Pefferkorn 1993; Pefferkorn 1995; Pefferkorn and Stoll 1990). Thus, the present results strongly suggest that, when studying NPs aggregation processes in the presence of FAs, the interaction of FAs with NPs can be considered as instantaneous compared to the aggregation processes. The results and conclusions reported here should be considered as a first step for several reasons. Indeed the presence of biopolymers in aquatic systems, monovalent and multivalent salt, as well as natural inorganic colloids, may also significantly modify the final stability, transport, and transformation processes of manufactured nanoparticles in aquatic systems.

Acknowledgments We gratefully acknowledge the financial support received from the Swiss National Science Foundation, Research Project 200021-135240. The authors would like to thank Prof. P. Le Coustumer (Bordeaux University) for his support during the characterization of the FAs and hematite nanoparticles.

References

Aiken GR (1985) Humic substances in soil, sediment, and water: geochemistry, isolation, and characterization. Wiley, New York

Amal R, Raper J, Waite T (1992) Effect of fulvic acid adsorption on the aggregation kinetics and structure of hematite particles. J Colloid Interface Sci 151:244–257. doi:10.1016/0021-9797(92)90255-K

Averett RC (1995) Humic substances in the Suwannee river, interactions, properties, and proposed structures. United States Geological, Georgia

Baalousha M (2009) Aggregation and disaggregation of iron oxide nanoparticles: Influence of particle concentration, pH and natural organic matter. Sci Total Environ 407:2093–2101. doi:10.1016/j.scitotenv.2008.11.022

Baalousha M, Manciulea A, Cumberland S et al (2008) Aggregation and surface properties of iron oxide nanoparticles: influence of pH and natural organic matter. Environ Toxicol Chem 27:1875–1882. doi:10.1897/07-559.1

Buffle J, Chalmers RA, Masson MR, Midgley D (1988) Complexation reactions in aquatic systems: an analytical approach. E. Horwood, Chichester

Buffle J, Wilkinson KJ, Stoll S et al (1998) A generalized description of aquatic colloidal interactions: the three-colloidal component approach. Environ Sci Technol 32:2887–2899

Carnal F, Stoll S (2011) Adsorption of weak polyelectrolytes on charged nanoparticles. Impact of salt valency, pH, and nanoparticle charge density. Monte Carlo simulations. J Phys Chem B 115:12007–12018. doi:10.1021/jp205616e

Chen KL, Mylon SE, Elimelech M (2006) Aggregation kinetics of alginate-coated hematite nanoparticles in monovalent and divalent electrolytes. Environ Sci Technol 40:1516–1523. doi:10.1021/es0518068

Cross KM, Lu Y, Zheng T et al (2009) Water decontamination using iron and iron oxide nanoparticles. Nanotechnol Appl Clean Water 347–364

Ferretti R, Stoll S, Zhang J, Buffle J (2003) Flocculation of hematite particles by a comparatively large rigid polysaccharide: schizophyllan. J Colloid Interface Sci 266:328–338. doi:10.1016/S0021-9797(03)00527-7

Fidler MC, Walczyk T, Davidsson L et al (2004) A micronised, dispersible ferric pyrophosphate with high relative bioavailability in man. Br J Nutr 91:107–112

Gupta AK, Gupta M (2005) Synthesis and surface engineering of iron oxide nanoparticles for biomedical applications. Biomaterials 26:3995–4021. doi:16/j.biomaterials.2004.10.012

He YT, Wan J, Tokunaga T (2007) Kinetic stability of hematite nanoparticles: the effect of particle sizes. J Nanopart Res 10:321–332. doi:10.1007/s11051-007-9255-1

Jones MN, Bryan ND (1998) Colloidal properties of humic substances. Adv Colloid Interface Sci 78:1–48. doi:16/S0001-8686(98)00058-X

Ju-Nam Y, Lead JR (2008) Manufactured nanoparticles: an overview of their chemistry, interactions and potential environmental implications. Sci Total Environ 400:396–414. doi:10.1016/j.scitotenv.2008.06.042

Kadar E, Simmance F, Martin O et al (2010) The influence of engineered Fe_2O_3 nanoparticles and soluble ($FeCl_3$) iron on the developmental toxicity caused by CO_2-induced seawater acidification. Environ Pollut 158:3490–3497. doi:10.1016/j.envpol.2010.03.025

Kosmulski M (2002) The pH-dependent surface charging and the points of zero charge. J Colloid Interface Sci 253:77–87. doi:10.1006/jcis.2002.8490

Liang L, Morgan JJ (1990) Coagulation of iron oxide particles in the presence of organic materials: application of surface chemical model. ACS Symposium Series, American Chemical Society, Washington DC 416:293–308

Maurice PA, Namjesnik-Dejanovic K (1999) Aggregate structures of sorbed humic substances observed in aqueous solution. Environ Sci Technol 33:1538–1541. doi:10.1021/es981113+

Murphy EM, Zachara JM, Smith SC (1990) Influence of mineral-bound humic substances on the sorption of hydrophobic organic compounds. Environ Sci Technol 24:1507–1516. doi:10.1021/es00080a009

Ouali L, Pefferkorn E (1993) Polymer induced stabilization of colloids mechanism and kinetics. J Colloid Interface Sci 161:237–246. doi:10.1006/jcis.1993.1462

Pefferkorn E (1995) The role of polyelectrolytes in the stabilisation and destabilisation of colloids. Adv Colloid Interface Sci 56:33–104

Pefferkorn E, Stoll S (1990) Cluster fragmentation in electrolyte induced aggregation of latex. J Chem Phys 92:3112–3117. doi:10.1063/1.457910

Perez JM (2007) Iron oxide nanoparticles: hidden talent. Nat Nano 2:535–536. doi:10.1038/nnano.2007.282

Piccolo A (2001) The supramolecular structure of humic substances. Soil Sci 166:810–832. doi:10.1097/00010694-200111000-00007

Santschi PH (1984) Particle flux and trace metal residence time in natural waters. Limnol Oceanogr 29:1100–1108

Schwertmann U, Cornell RM (1991) Iron oxides in the laboratory—preparation and characterization. VCH, Weinheim

Seijo M, Ulrich S, Filella M et al (2009) Modeling the adsorption and coagulation of fulvic acids on colloids by Brownian dynamics simulations. Environ Sci Technol 43:7265–7269. doi:10.1021/es9002394

Shipley HJ, Engates KE, Guettner AM (2010) Study of iron oxide nanoparticles in soil for remediation of arsenic. J Nanopart Res 13:2387–2397. doi:10.1007/s11051-010-9999-x

Stemmler SJ, Berthelin J (2003) Microbial activity as a major factor in the mobilization of iron in the humid tropics. Eur J Soil Sci 54:725–733. doi:10.1046/j.1351-0754.2003.0571.x

Stumm W, Morgan JJ (1996) Aquatic chemistry: chemical equilibria and rates in natural waters. Wiley, New York

Tipping E, Higgins DC (1982) The effect of adsorbed humic substances on the colloid stability of haematite particles. Colloids Surf 5:85–92. doi:10.1016/0166-6622(82)80064-4

Watts RJ, Jones AP, Chen P-H, Kenny A (1997) Mineral-catalyzed fenton-like oxidation of sorbed chlorobenzenes. Water Environ Res 69:269–275

Waychunas GA, Kim CS, Banfield JF (2005) Nanoparticulate iron oxide minerals in soils and sediments: unique properties and contaminant scavenging mechanisms. J Nanopart Res 7:409–433. doi:10.1007/s11051-005-6931-x

Zhang W (2003) Nanoscale iron particles for environmental remediation: an overview. J Nanopart Res 5:323–332. doi:10.1023/A:1025520116015

Zhang J, Buffle J (1995) Kinetics of hematite aggregation by polyacrylic acid: importance of charge neutralization. J Colloid Interface Sci 174:500–509. doi:10.1006/jcis.1995.1417